

Military Technical College
Kobry Elkobbah, Cairo,
Egypt.



3rd International Conference
On
Chemical & Environmental
Engineering

PURIFICATION OF UNDERGROUND WATER FROM FERROUS AND MANGANOUS IONS USING ACTIVATED CARBON DERIVED FROM RICE HUSK (CASE STUDY)

Diafullah A. A.^{*}, Abdo. M. H.^{**}, Moustafa M. E.^{***},
Amin A. S.^{***} and Mohamed F. M.^{****}

ABSTRACT

To address questions of water quality and to suggest a local and available treatment process for iron and manganese removal, ground water samples were collected at 4-stations (I, II, III, IV) seasonally during March 2003 - Feb. 2004 and determined using atomic absorption spectrophotometer (AAS). The results showed that the concentrations of these ions are higher than the permissible levels. In this concern, treatment procedure was evaluated using activated carbon prepared by chemical activation of rice husk using 70 % H₃PO₄ at 500 °C. Factors affecting adsorption process (e.g. contact time and sorbent mass) were examined. The results showed that the percent removal almost reaches ≥ 99 % and in all cases the ion concentration after treatment is less than the permissible level. Adsorption isotherm indicates that the monolayer coverage is 0.357 g and 0.625 g of ferrous and Manganous per gram of sorbent respectively. In dynamic mode, the adsorption capacity (i.e., $C_e/C_o = 50$ % or $Q_{0.5}$) was 1 mg/g at flow rate 1liter/min. and the column recycled at least five times and only needed 1/ 2 ml of KMnO₄ (0.06M) for each regeneration step and no loss in sorbent per cycle should be considered. Therefore, activated carbon derived from rice husk may be considered as a better replacement technology for removal of Fe⁺² and due to good efficiency in this application. The possible working adsorption mechanisms are discussed and confirmed by FTIR.

KEY WORDS

Purification, modified rice husk, under ground water, adsorption, ferrous, manganous ions and activated carbon.

* Hot Lab. Center, Atomic Energy Authority,

** National Institute of Oceanography and Fisheries.

*** Faculty of Science, Banha University,

**** Kaha Company for Chemical Industries, National Authority for Military Production.

1. INTRODUCTION

According to figures recently issued by the world health organization, (WHO) an average of 50000 people die each day from diseases associated with bad water; one person about every two second [1].

Drinking water can come from either ground water sources (via wells) or surface water sources (such as river, lakes, and streams).

Iron and Manganese are common in groundwater supplies and the maximum contaminant levels (MCL) according to WHO is 0.3 mg/l and 0.1mg/l of iron and manganese respectively [1-8].

Neither iron nor manganese poses health risks. Both in small concentrations are essential of human health. But the presence of significant iron and manganese in water supplies can create several problems: (i) Long time consumption of drinking water with high concentration of iron causes liver diseases, (ii) Higher concentration will give a water a medicinal or metallic taste, (iii) Cause corrosion and pipe blockages either directly, precipitating deposits or indirectly by providing favorable condition for growth of specific bacteria [3], (iv) Large concentrations of iron and manganese in water can cause troubles in domestic and industrial uses and (v) In extreme cases, iron and manganese interfere with culinary use, turning tea black and darkening boiled vegetables [3,4]

Because iron and manganese are chemically similar, they cause similar problems. Iron will cause reddish-brown staining of laundry, porcelain, dishes, utensils, and even glassware. Manganese acts in a similar way but causes a brownish-black stain. Soaps and detergents do not remove these stains, and the use of chlorine bleach and alkaline builders (such as sodium carbonate) can actually intensify the stains [3,4]. Iron and manganese accumulations become an economic problem when water supply or softening equipment must be replaced. There are also associated increased energy costs, like pumping water through constricted pipes or heating water with heating rods coated with iron or manganese minerals.

There are many methods of iron and manganese removal (9-14): polyphosphate treatment that protect dissolved iron and manganese from reacting with oxygen and precipitate by trapping them in a complex molecule that is soluble in water, (ii) soluble iron and manganese can be exchanged for sodium on an exchange resin or zeolite, (iii) greensand filtration using the active Glauconate mineral. This clay mineral will form insoluble iron and manganese and it must be regenerated by KMnO₄ for frequent uses, and (iv) chemical oxidation followed by filtration is accepted method of iron and manganese removal. In this concern, soluble iron and manganese begin to precipitate after contact 20 min. with chlorine solution (oxidant). An additional advantage of using chlorination system is bacteria damage.

Concentration of iron and manganese when using the aforementioned methods of treatment is as follows: polyphosphate treatment (0-3 ppm); ion-exchange (softener) (0-10 ppm); Greensand filter (0-10 ppm) and chlorination (0 - > 10 ppm).

Approximately 100 million tones of rice husk is available annually for utilization in developing countries. However, the amount of rice husk available is far in excess of any local uses and thus has posed a disposal problem (15).

Rice husk was chosen as an adsorbent in several water treatment processes due to suitable structure, insolubility in water, chemical stability, high mechanical strength and its local availability at almost no cost.

In the present study, a new method was suggested for iron and manganese removal from groundwater using activated carbon prepared from rice husk by chemical activation with 70% H₃PO₄ and heat treatment at 773K. Factors affecting sorption process are studied in batch and column modes.

2. EXPERIMENTAL

i- Experimental design: The experimental part is divided into two main sections:

(i) the 1st concerns with the regular routine analysis of the ground water samples in the four stations before and after traditional treatment. (ii) the 2nd section concerns with the removal of Fe and Mn ions of a representative sample obtained from station I. Whereas, the treatment is depended on adsorption technique using activated carbon prepared from Rice Husk.

ii. Sampling: The sampling period form March 2003 to Feb. 2004. groundwater samples were collected seasonally from four stations as presented in Fig. 1 the capacity of each station is approximately 10,000 m³/day. The groundwater samples were kept in well stoppered polyethylene plastic bottles (1 L capacity) and taken the notations I, II, III and IV before treatment and I', II', III' and IV' after treatment.

iii. Preparation of activated carbon: Rice Husk was chosen as a precursor for the preparation of active carbon by impregnation with 70% H₃PO₄. The temperature was raised at the rate of (50 °C/ 5 min.) up to 500°C and hold at this temperature for 2.5 h. This carbon was taken RH-57 as notation.

iv. Treatment procedures: Factors affecting the adsorption process e.g. equilibrium time, batch factor, sorbent mass were studied. In all cases, 1 L of ground water was contacted with 0.008 g of AC in stoppered bottle. The conditions of each experiment were adjusted, then, the mixture was filtered and the samples were analyzed for iron and manganese concentration using AAS. Isotherm experiments were carried out using bottle point technique. Each sample was mixed with various quantities of AC ranging from 0.002 to 0.01 g and agitated for 4 hrs in case of iron and 5 hrs in case of manganese at room temperature (25 ± 1°C). The concentration was measured in the filtrate using AAS (model: ZL8100 Schmitzu).

In all cases, the difference between the initial concentration (C^o) and the equilibrium concentration (C_e) was calculated and used to determine the adsorptive capacity (q_e) as follows: $q_e = V(C^o - C_e) / M$, Where V is the total volume of solute solution (l), M the mass of adsorbent used (g), C^o the initial concentration of the solute (g l⁻¹), and C_e is the residual concentration of the solute (g. ⁻¹)

RESULTS AND DISCUSSION

1st section: The data listed in tables (1-4) describe the concentration levels of the physicochemical in (ppm) of the 4- stations (I, II, III and IV) in the four seasons. Traditional treatment technique in the four stations was applied (aeration, oxidation, filtration and chlorination) and aimed to reduce the concentration of iron and manganese only to the permissible limits (1 and 0.5 ppm) respectively. But, it is well known that groundwater is not stable like surface water so the concentration of the constituents are varied seasonally. This variation is dependant on the solubility of

these constituents and contamination of groundwater by rain and industrial wastewaters. As shown in tables (1-4), all parameters before and after treatment are cited within normal limits according to WHO and Egyptian specification except the following parameters:

- 1- iron and manganese levels before treatment exceeded the permissible levels and thus treatment is a must.
- 2- Lead is out of limits (more than 0.05 mg/l) in all stations at all seasons except station IV in the all seasons, station I at the autumn.
- 3- Iron and manganese after treatment are within limit of Egyptian specification except for manganese in station IV at the summer season.
- 4- TDS before and after treatment are within the normal limits (1200 mg/l) except for station IV at all seasons. This may be due to contamination of wells with fertilizers and some industrial pollutants.
- 5- Similar observation is recorded for TS in station IV in the autumn and winter seasons.

The 2nd section :

The physicochemical properties of RH-57 are presented in table 5. The pore size distribution by DFT is presented in Fig.2 and it shows a significant amount of micropores with the apparent bimodal distribution of pores in the microporous region with maxima at 1.1 and 1.7 nm respectively. The density function theory (DFT) method is applicable for the entire range of pore sizes accessible by the adsorptive molecule (N₂), which makes this technique very attractive compared to the commonly used BET method (16). The surface area and pore volume of RH- 57 are 419 m²/g and 0.213 ml/g respectively.

Adsorption Experiments:

Effect of agitation time: The time –profile of adsorption of Fe²⁺ and Mn²⁺ ions onto RH- 57 at room temperature (25 ±1°C) is presented in Fig.3. Agitation time increases, cation removal also increases initially, but then gradually approaches a constant value, denoting attainment of an equilibrium. Obviously, the equilibrium was attained after shaking for about 4 h in case of Fe²⁺ and 5 h in case of Mn²⁺, beyond which there is no further increase in the adsorption. As shown in Fig.3, the uptake amount increased 100 to 400 mg/g in case of Fe²⁺ and from 40 to 500 mg/g in case of Mn²⁺ to reach the equilibrium. A shaking time of 5h employed for all the equilibrium adsorption studies was enough to ensure that adsorption equilibrium was reached in each case.

Sorption Dynamics:

Rate constant study:

The kinetics of sorption of selected metal ions under investigation on carbon were studied on the basis of Lagergren equation (17):

$$\text{Log } (q_e - q) = \text{log } q_e - (K_{ad} / 2.303) t \quad (1)$$

Where q (mg/g) is the amount of metal ions sorbed at time t , q_e (mg/g) is the amount sorbed at equilibrium and K_{ad} is the equilibrium rate constant of sorption. The straight line plots (Fig.4) of $\text{log } (q_e - q)$ vs. t for the two metal ions indicate the validity of

equation (1) and the process follows first order rate kinetics. The K_{ad} values of metal ions were calculated from slopes of these plots and the results are given in Table 6.

Diffusion rate constant study:

In the model developed by Weber and Morris (1963), the rate of intra-particle diffusion is a function of $t^{0.5}$ and can be defined as follows (17):

$$q_t = k_p t^{0.5} \tag{2}$$

The intra-particle diffusion rates (k_p) were determined by plotting the amount sorbed per unit weight of sorbent (q_e) vs. $t^{1/2}$, as shown in Fig. 5. The sorption rates for intraparticle diffusion, K_p were calculated from the slopes of the linear portions of the respective plots with units of $mg.g^{-1} min^{-0.5}$ (not the true reaction rate, but relative rates which are useful for comparative purposes) and are given in Table 6. The two plots have the same general features, initial curved portion followed by linear portion and plateau. The initial curve portions are attributed to the boundary layer diffusion effects. While the linear portions are a result of the intraparticle diffusion effects (17) and the plateau is attributed to the equilibrium. An extrapolation of the linear portion of the plots back to the time^{0.5} axis provides intercepts which are proportional to the extent of boundary layer thickness. The larger the intercept, the greater is the boundary layer effect (17), and it follows the sequence: $Mn^{2+} > Fe^{2+}$. This follows the same order of ionic radius as shown in Table 6.

Effect of sorbent mass: Fig. 6 shows that increasing the carbon concentration increases the percent removal (R%) to reach 100 % from 1L solution containing initial concentrations of 2, 3 mg/l of Fe^{2+} and Mn^{2+} respectively (sample of station I in winter) and attained constant removal after a particular carbon concentration (optimum dosage). The minimum adsorbent dosage of 8 mg was required for complete removal of either Fe^{2+} or Mn^{2+} after contact period of 5 hrs.

Adsorption isotherms: Adsorption data for a wide range of adsorbate concentrations are most conveniently described by adsorption isotherm such as the Langmuir or Freundlich isotherm, which related adsorption density q_e (metal uptake per unit weight of adsorbent) to equilibrium adsorbate concentration in the bulk fluid phase C_e . The langmuir isotherm is represented by the following equation:

$$c_e/q_e = 1/bq^0 + (c_e/b q^0) \tag{3}$$

where c_e is the equilibrium concentration (mg/l), q_e is the amount adsorbed at equilibrium time (mg/g) and q^0 and b are Langmuir constants related to adsorption capacity and energy of adsorption, respectively (18).

The linearized Langmuir plot is shown in Fig. (7). The Langmuir parameters were calculated using Eq. (3) and were found to be (357 g/g and 625 g/g for q^0) for iron and for manganese, respectively. The Freundlich adsorption isotherm was also applied for the adsorption of Fe^{2+} & Mn^{2+} ions onto RH-57. The Freundlich equation is presented (18) as:

$$q_e = k_f c_e^{1/n} \tag{4}$$

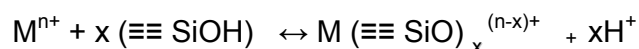
Rearranging Eq. (4) gives:

$$\text{Log } q_e = \text{log } k_f + 1/n \text{ log } c_e \tag{5}$$

Hence, a plot of $\log q_e$ vs. $\log c_e$ enables the constants k_f and exponent n to be determined as shown in Fig. (8). The constants are listed in Table 7. Although the correlation coefficients are greater than 95%, they do not correlate the data as well as the Langmuir isotherm, which has consistently higher correlation coefficients as seen in Table 7.

Possible working mechanism:

The ion-exchange reaction on the silica surface is accomplished through the substitution of protons of the surface silanol groups by the metal ions from solution, as follows (18):



Where M^{n+} = metal ion with $n+$ charge, $(\equiv \text{SiOH})$ = silanol group on the SiO_2 surface and $x\text{H}^+$ = number of protons released. The cation-exchange mechanism is expected with the two metal ions as the sorbent contains large amounts of silica (> 95%) in the ash content (31%).

Also, since electrostatic attraction was possible negatively charged adsorbent surface and positively charged metal ion species, it seems that some electrostatic forces were involved in the adsorption process (19).

According to surface chemistry theory, RH-57 particles and metal ions are both surrounded by an electric double layer due to electrostatic interactions (20). Based on the theory of the diffuse double layer, the thickness of the double layer is compressed by an increase in the ionic strength of the solution (21, 22). Such compression helps the carbon particles and metal ions to approach each other more closely. The attractive forces (such as van der Waals' forces) then become significant, leading to an increased uptake of metal ion.

Besides, two major types of chemical bindings can be responsible for the adsorption of the two metal ions onto the RH-57 carbon (23). The covalent bonding results from the sharing of the free electron pairs between the surface oxygen atom and the metal atom or the formation of an O-M bonding. The hydrogen bonding between surface oxygen atom and the hydrogen atom of the hydrated metal ions.

The FTIR was used to evaluate the mechanism involved. Fig. 9 shows FTIR spectra of RH-57 carbon (original), with Mn^{2+} ions and with Fe^{2+} ions. All the spectra showed the broad bands at 3425 and 1189 cm^{-1} which may be due to hydrogen bonded $-\text{OH}$ and $\text{P}=\text{O}$. Thus, the surface OH groups probably interact with water molecules adsorbed by the carbon surface from the environment (24). The high silica content appears in FTIR spectra, the presence of free SiO_2 indicated by the presence of peak at 477 cm^{-1} . The peak at 1100 cm^{-1} is very strong due to the presence Si-O asymmetric stretching bond. The peak at about 800 cm^{-1} is considered to be the bonding between C and Si or the overlapping of the Si and Si-OH vibrations (25-27). Also, the intensity of the peak near 3425 cm^{-1} , due to the Si-OH stretching, decreased after the uptake due to the interaction between the metal ion and the surface groups. The band in the region of 1260 cm^{-1} has been observed for RH-57 carbon and shifted to lower wave numbers with high intensity after metal removal. This band is due to stretching vibration of aromatic $\text{C}=\text{C}$ bond, which are polarized by oxygen atoms near one of the carbon atoms (28) or due to highly conjugated carbonyl groups (29). A new peak at 521 cm^{-1} appears in the spectrum of RH-57 with

Mn²⁺ which corresponds to Mn=O stretching mode. The peak at 1189 cm⁻¹ appears as shoulder after Fe²⁺ uptake with high intensity and the peak at 1096 cm⁻¹ is shifted to higher wave number (1107 cm⁻¹) with high intensity after Mn uptake. Similar trend was also observed when oil shale was treated by sodium and potassium hydroxide (30) due to metal carbonation and metal salt vibrational modes.

DYNAMIC STUDIES:

Fig. 10 Shows that the column filled with RH-57 carbon can be regenerated and recycled at least five times without affecting the sorption capacity of RH-57 for Fe²⁺ ions (with an initial concentration C^o = 2 ppm). Experimentally, similar service time of 5 min. (t_{1/2}) at 50% breakthrough was obtained even after five times of successive regeneration using 0.5 ml of 1% KMnO₄ 0.06 M concentration. The adsorption capacity was determined at this high flow rate (1l/min.) using column experiments data by integrating the upper part of concentration versus throughput volume (Fig.10). The adsorption capacity at C_e/C^o = 50% or Q_{0.5}) was 1 mg Fe²⁺ per 1 gram sorbent. The total integrated amount of Fe²⁺ adsorbate was divided by the weight of the sorbent placed in the column to yield the adsorption capacity of 1 mg/g. Since this capacity was quite lower than the Langmuir monolayer capacity (0.357 g/g) presented in table 7, it may be inferred that full saturation of the sorbent active sites was not achieved due to the limited time of equilibrium due to the high flow rate (one liter/min.) used under dynamic column conditions. Another factor causing the discrepancy may be the partial invalidity of the Langmuir assumption, i.e., envisaging monoenergetic adsorption on a homogeneous surface, on the inhomogeneous surface of the RH-57 as a composite sorbent. As shown in Fig.11, the column needs only 0.5 ml of 0.06 M KMnO₄ for each cycle and no weight loss per cycle should be considered.

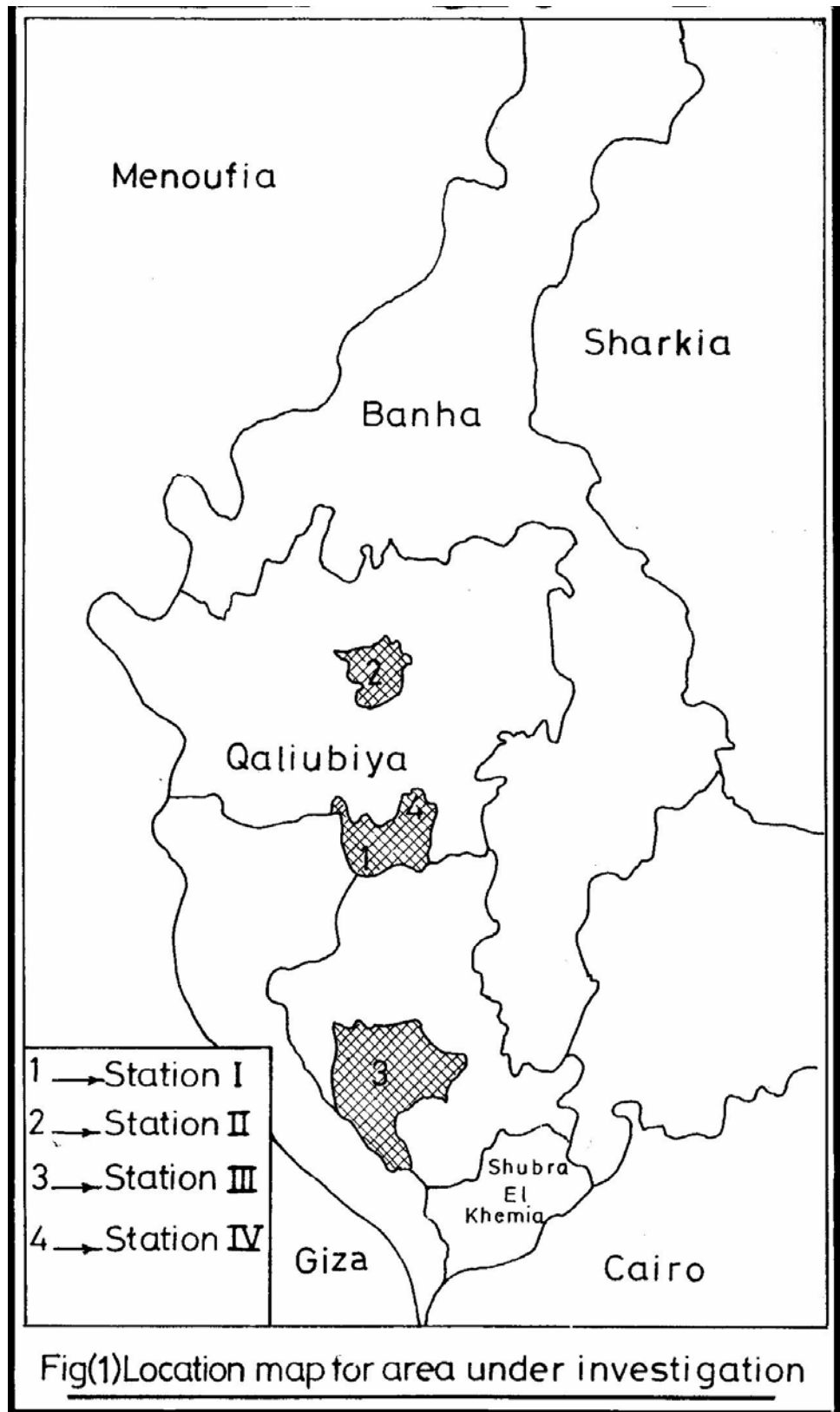
RECOMMENDED PROCEDURES:

Removal of iron and manganese ions in the treatment of ground water samples using RH-57 carbon derived from chemical activation of rice husk is significant and meaningful and can be addressed due to: i)- low cost; ii) easy operated; iii) high efficiency; iv) solve disposal problem of agro-residue (rice husk). The physicochemical parameters of ground water sample obtained from station I, before and after treatment by RH-57 was presented in table10, which prove that the quality of the water is improved and the iron and manganese ions are completely removed.

REFERENCES

- [1] Introducing of groundwater, Michael, Price, Chapaman, Hall 1991-1992
- [2] Water Treatment Hand Book- Fifth edition- Degremont 1979.
- [3] Hand book McGraw- Hill New York. (Water quality and treatment), 4th (1990).
- [4] American Water Works Association Water Quality and Treatment, 4th (1998).
- [5] American Water Works Association Water Quality and Treatment, 4th (2000).
- [6] Guidelines for Drinking Water Quality, WHO, Geneva, (2003).
- [7] Ground Water, Drinking Water, U.S .Environmental Protection agency, (2004).
- [8] National Research Council, Safe Water from Every Tap: Improving Water Service to Small Communities, National Academy Press, Washington DC (1997).
- [9] S.D. Faust and J. V. Hunter, Principles and applications of water chemistry, John Wiley and Sons, Inc. New York, pp. 625- 643 (1967).

- [10] R. E. Machmeir, Iron in Drinking water, AG-FO-138, Minnesota Extension Service, University of Minnesota, Agriculture (1990).
- [11] M. E. Flentje and R. J. Faust (ed.), Water quality and treatment- a handbook of public water supplies, 3rd Edition. Prepared by The American Treatment Systems for Household Water Supplies—Iron and Manganese Removal, pp. 380-396 (1971).
- [12] V. L. Snoeyink, and D. Jenkins, Water Chemistry. John Wiley and Sons, Inc., New York (1980).
- [13] Water Quality Association Recommended industry standards for household and commercial water filters-a voluntary standard, S-200. National Headquarters and Laboratory, Lisle, Illinois (1988).
- [14] Water Quality Association Recongized treatment technique for water regulations with the application of point- of- use system, R28, National Headquarters and Laboratory, Lisle, Illinois (1989).
- [15] A.A.M.Daifullah, B.S.Girgis and H.M.H.Gad "Utilization of agro-residues (rice Husk) in small wastewater treatment plans, Materials Letters 57 (2003), pp. 1723 -1731
- [16] J. Byrne, H.Fmarsh, In " Porosity in carbons: characterization and applications" (J.W. Patrick, Ed), Edward Arnold, London, p. 1. (1995).
- [17] H.H. Tran, F.A. Roddick, J. A. O'Donnell, Comparison of chromatography and desiccant silica gels for the adsorption of metal ions-I. Adsorption and Kinetics, Wat. Res. 33, No.13, (1999), pp. 1992-1997.
- [18] W.J. Weber Jr., Physicochemical Processes for Water Quality Control, Wiley, New York, 1972 (chapter 5).
- [19] C. Namasivayam, K. Ranganathan, Removal of Cd (II) from wastewater by adsorption on "waste" Fe(III)/Cr(III) hydroxide, Wat. Res. 29 (1995) pp.1737 – 1744.
- [20] M.A. Osipoowl, Surface Chemistry, Marcel Dekker, New York, 1972.
- [21] M.A. Rashid, D.E. Buckley and K.R. Robertson, Geoderma, 1972, 8, p. 11.
- [22] G.Müller, C.J. Radke and J.M. Prausnitz, J. Phys. Chem. ,1980, 84, p. 369
- [23] M.O. Corapcio and C.P. Huang, The adsorption of heavy metals onto hydrous activated carbon, Water Research 21 (9) (1987) pp. 1031 – 1044.
- [24] F. Stoeckli, A. Lavanchy, Carbon 38 (2000) p. 475.
- [25] B. Stuart, "Modern Infrared Spectroscopy" John Wiley & Sons, New York (1996).
- [26] B. K. Padhid C. Patnaikb, " Development of Si₂-N₂O, Si₃N₄ and SiC ceramic materials using Rice Husk" Ceramics International 21 (1995), pp. 213- 220.
- [27] D.M. Ibrahim, S.A. El-Hemaly and F.M. Abdel-Kerim " Study of Rice Husk Ash Silica by Infrared Spectroscopy" Themochimica Acta, 37 (1980), pp. 307- 314.
- [28] B.K. Pradhan and N.K. Sandles " Effect of different oxidizing agent treatments on the surface properties of activated carbon" Carbon 37 (1999), pp. 1323- 1332.
- [29] A. H. El-Sheikh, A.P.Newman, H.K.Al-Daffae, S. PN. Cresswell, "Characterization of activated carbon prepared from a single cultivar of Jordanian Olive stones by chemical and physicochemical techniques" J. Anal. Appl. Pyrolysis 71 (2004), pp. 151- 164.
- [30] R.A. Shawabkeh" Synthesis and characterization of activated carbo-aluminosilicate material from oil shale" microporous and mesoporous materials 75 (2004), pp. 107 – 114.



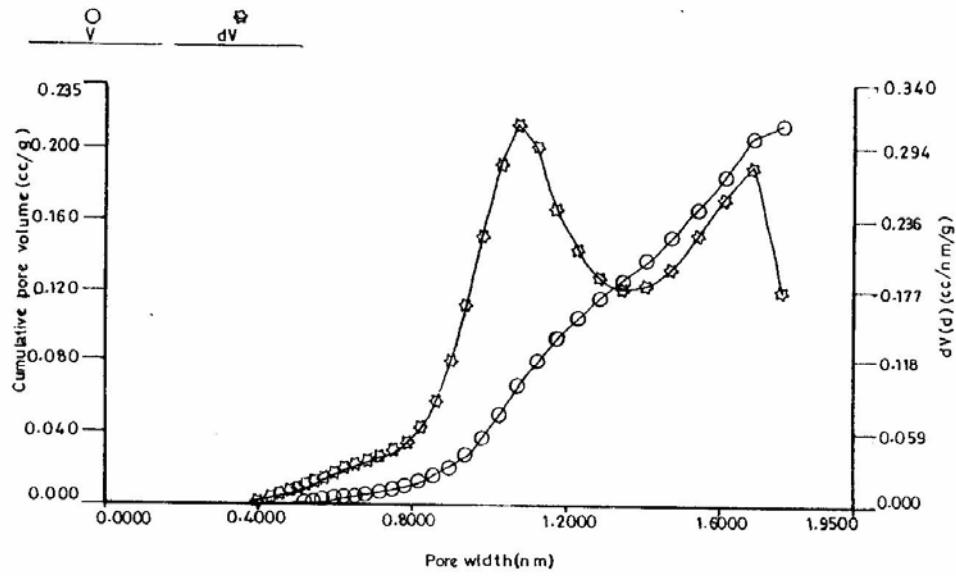
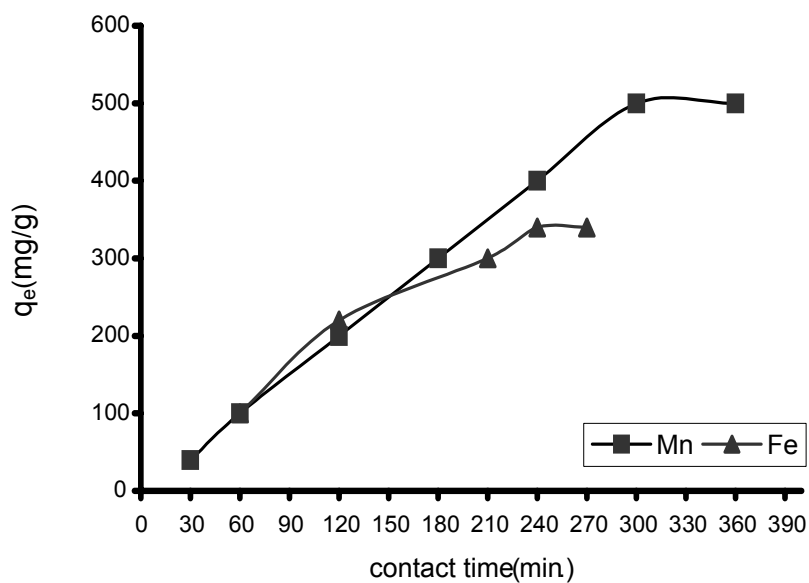
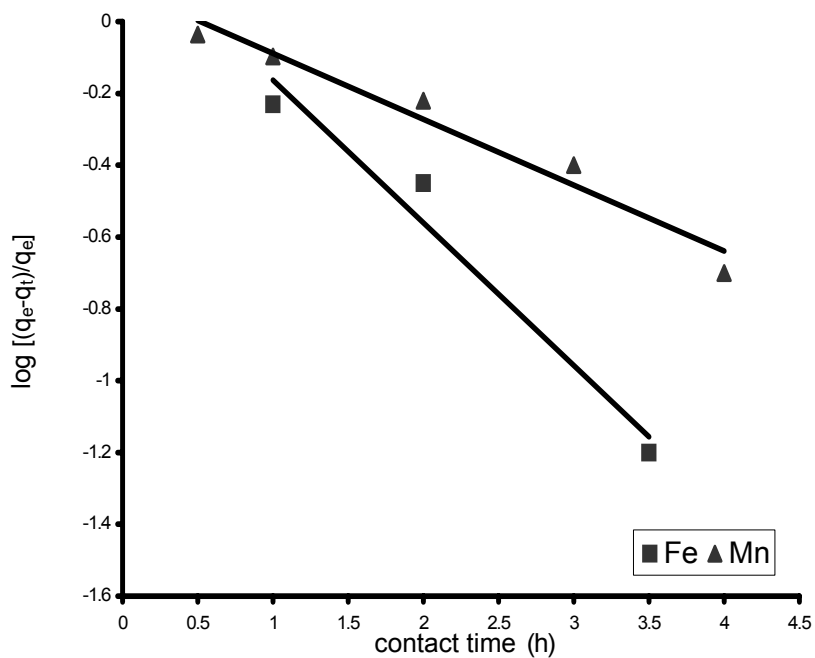


Fig. (2) the pore size distribution by DFT of RH-57 carbon

Fig(3) The sorbent phase concentration of RH-57 as a function of time for Fe²⁺ and Mn²⁺ removal



Fig(4) The sorbent phase concentration of MRH-57 (mg/g) as a function of time (h) for Fe²⁺ and Mn²⁺ removal



Fig(5)The sorbent phase concentration of MRH-57 (mg/g) as a function of time (h) for Fe²⁺ and Mn²⁺ removal

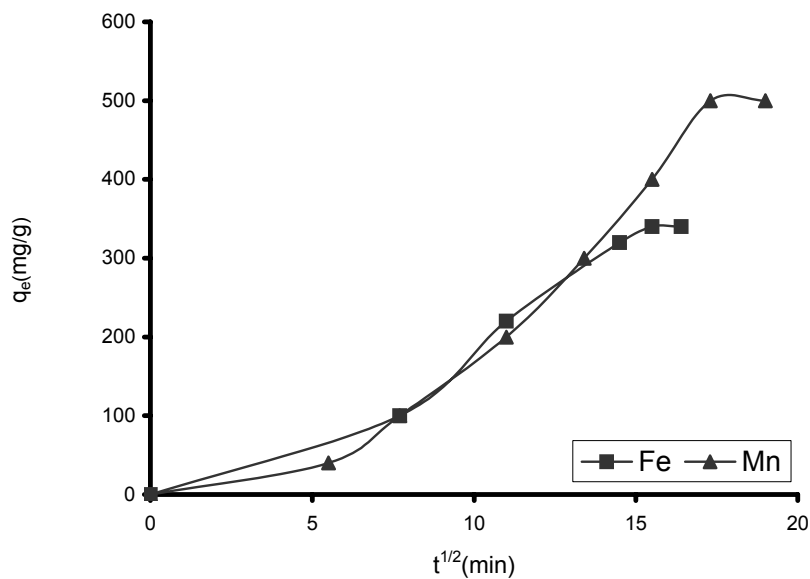
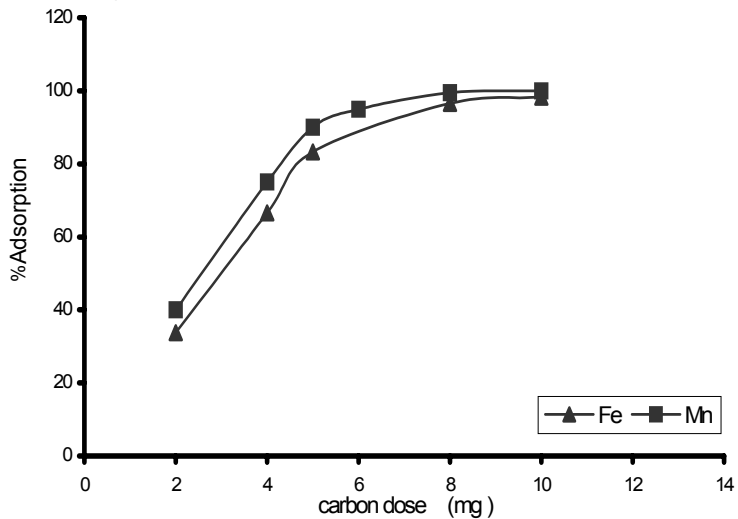
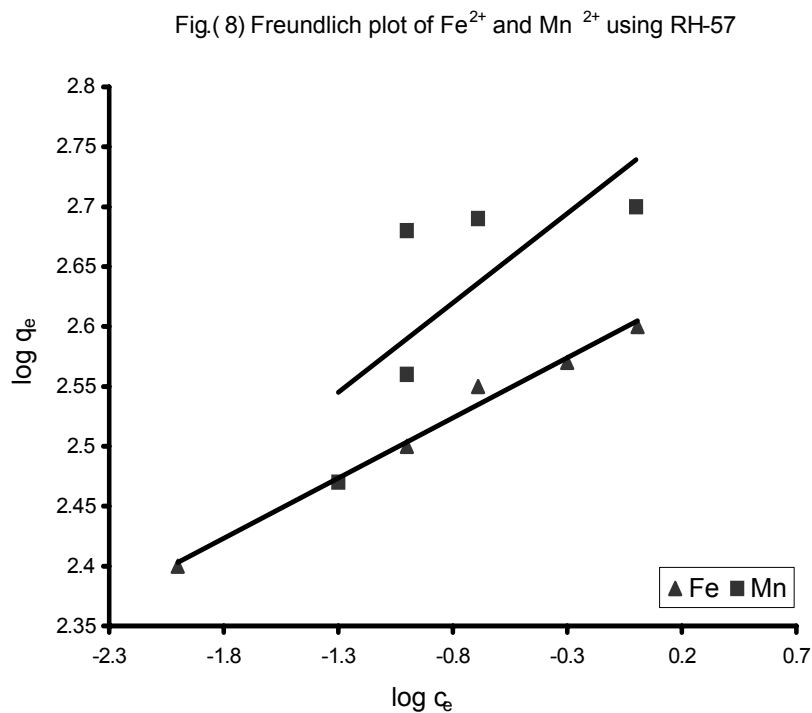
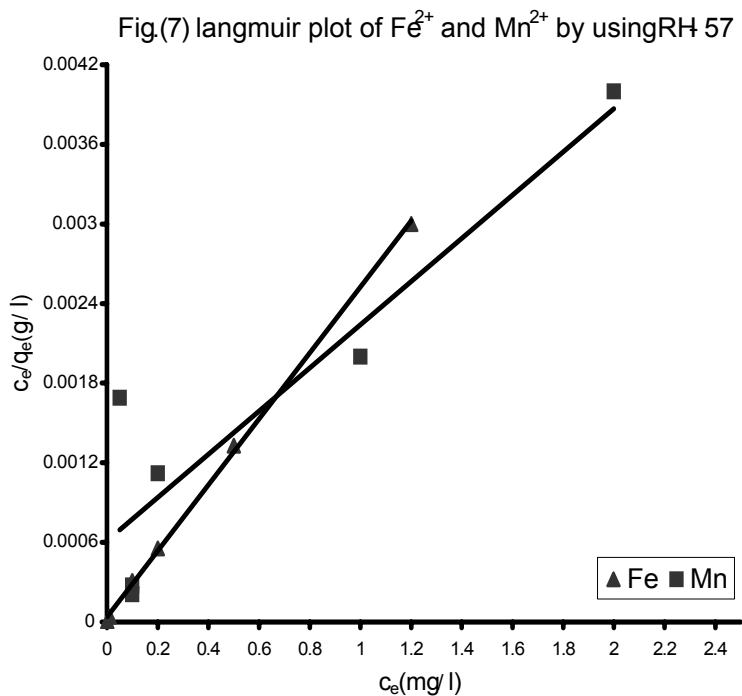


Fig (6)effect of Carbon dose on the adsorption of Fe²⁺ and Mn²⁺





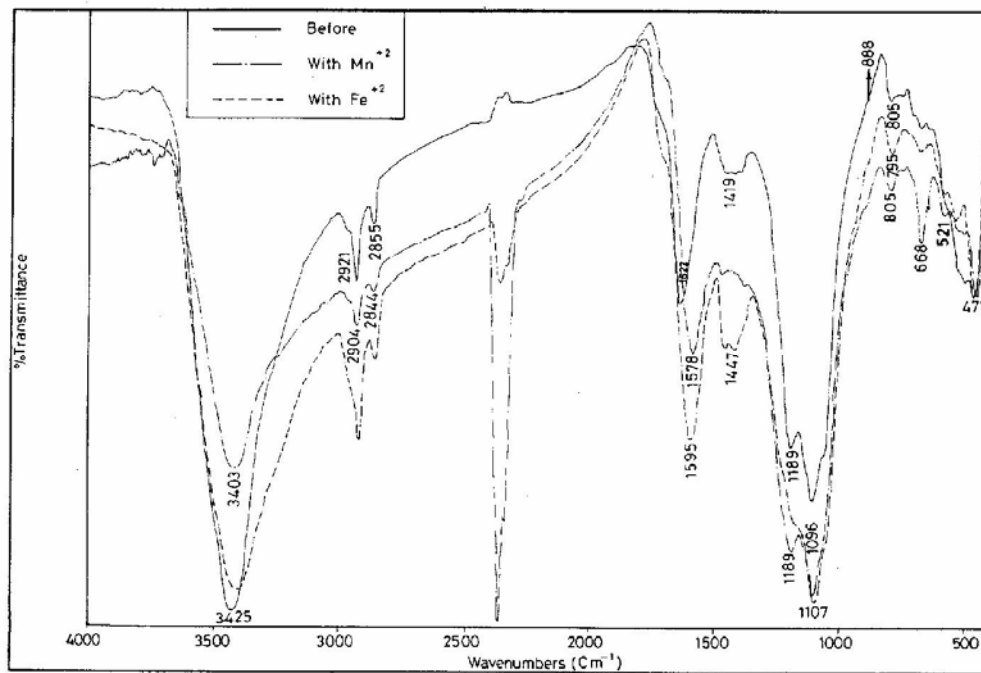


Fig (9) IR-spectra of RH-S7 carbon before and after uptake of Fe²⁺ or Mn²⁺

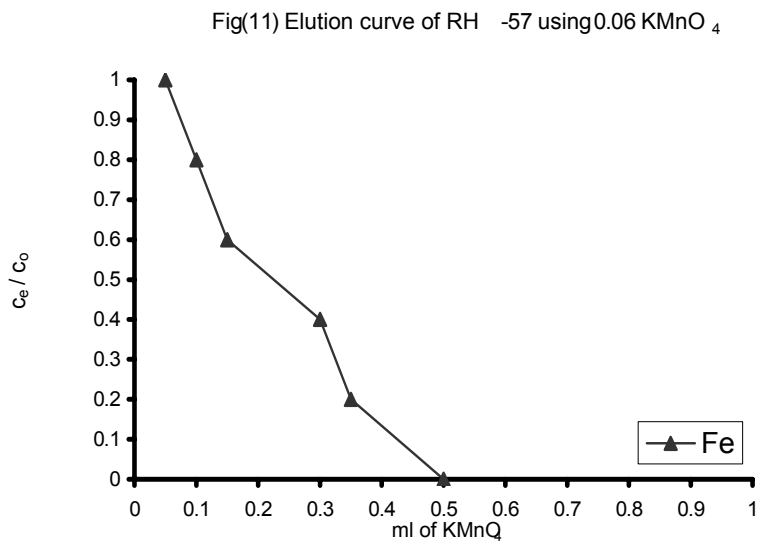
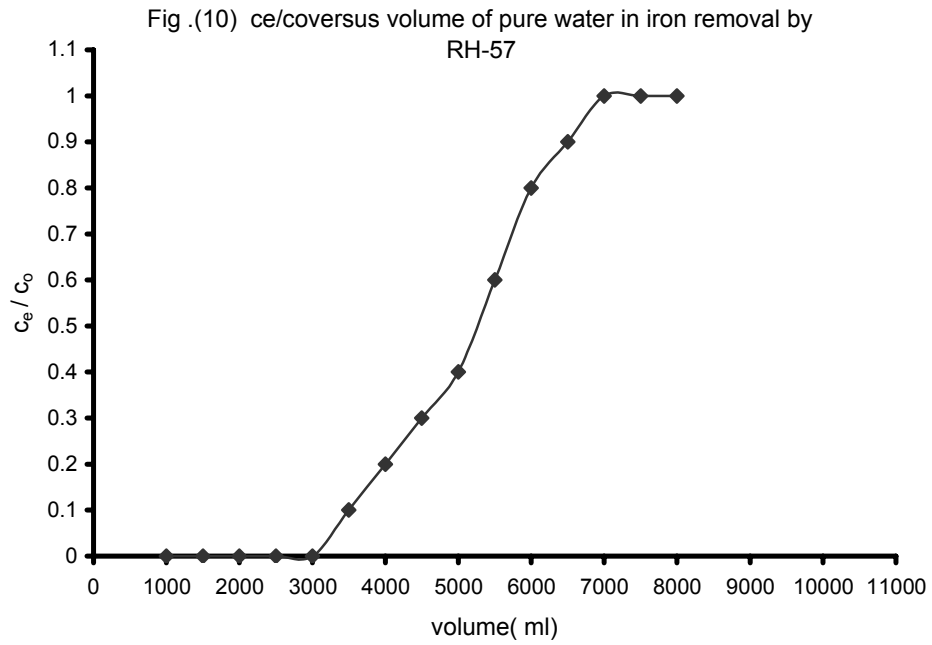


Table 5: The physicochemical parameters of RH-57

parameter	value
S _{BET} (surface area, m ² /g)	419
V _p (total pore volume, cm ³ /g)	0.213
d (pore width, nm)	1.076
ash content (%)	31
pH	3.5
Apparent density, g/cm ³	0.25
Packed density, g/cm ³	0.33
Grain size	0.6 mm

Table 6. Sorption Kinetic parameters of Fe⁺² and Mn⁺² ions using RH-57

Ionic radius (A)	K _p (mg.g ⁻¹ .min. ^{-0.5})	K _{ad} (min. ⁻¹)	Metal ions
0.76	0.0322	0.0097	Fe ⁺²
0.80	0.021	0.00306	Mn ⁺²

Table 7. Langmuir and Freundlich constants of Fe⁺² and Mn⁺² ions using RH-57

Adsorption system	Langmuir constants			Freundlich constants		
	q ^o	b	r	K _f	n	r
Fe ⁺² : RH ⁻⁵⁷	357	363	98.8	178	25.4	99.7
Mn ⁺² : RH ⁻⁵⁷	625	65	90.4	352	10.8	73.1

Table(8) The physico-chemical parameters in (mg/l) of ground water of station I (winter season) before and after treatment using RH-57 carbon compared to standard specifications

Parameter	TDS mg/l	pH	Heavy Metals				anions				Cations			
			Fe mg/l	Mn mg/l	Pb mg/l	Zn mg/l	SO ₄ ²⁻ Mg/l	Cl ⁻ mg/l	HCO ₃ ⁻ mg/l	CO ₃ ⁻ mg/l	Ca ²⁺ mg/l	Mg ²⁺ mg/l	Na ⁺ mg/l	K ⁺ mg/l
(a)	783	7.5	2	3	0.1	0.5	80.3	129.9	567.1	3.1	83.5	110.2	54.7	9.3
(b)	750	7.4	0	0	n.d	n.d	77	125	550	3.4	76	115.3	55.7	9
Specification														
Egyptian standard	1200	6.5-9.5	1	0.5	0.05	5	400	500	n.d	n.d	200	150	200	n.d
WHO	1200	6.5-8.5	0.3	0.1	0.05	5	400	250	n.d	n.d	n.d	n.d	200	n.d
European Standard	n.d	6.5-8.5	0.3	0.05	0.05	3	25	25	n.d	n.d	n.d	n.d	150-175	12
US Standard	500	6.5-8.5	0.3	0.05	0.05	5	250	250	n.d	n.d	n.d	n.d	n.d	n.d

a = before treatment
 b = after treatment using RH-57
 n.d = not detected